J Supercond Nov Magn (2012) 25:2187–2191
DOI 10.1007/s10948-012-1647-5

ORIGINAL PAPER

Superconducting Vortex Pinning with Magnetic Dots: Does Size and Magnetic Configuration Matter?

Axel Hoffmann · Pedro Prieto · Vitali Metlushko · Ivan K. Schuller

Received: 1 September 2011 / Accepted: 31 January 2012 / Published online: 4 July 2012

Abstract The pinning of superconducting vortices in type-II superconductors has been studied for a long time due to the wide variety of unusual flux flow phenomena and more importantly, for its relevance in applications, since vortex pinning is one of the essential parameters controlling the enhancement of critical currents. A case of particular interest is the use of artificial magnetic pinning centers, since they can be fabricated to match well the characteristic length scales relevant for superconductivity and their magnetization offers another degree of freedom to influence the pinning properties. This article reviews our work on the role of the size and separation of the magnetic dots. Furthermore, we also show that the magnetic configuration can influence significantly the pinning strength, through the magnetic stray fields penetrating the superconductor, which can be drastically different.

Keywords Superconducting vortices · Magnetic vortices · Periodic pinning · Magnetotransport

A. Hoffmann (✉)
Materials Science Division, Argonne National Laboratory, Argonne, IL 60439, USA
e-mail: hoffmann@anl.gov

P. Prieto
Universidad del Valle, Cali, Colombia

V. Metlushko
Electrical and Computer Engineering, University of Illinois at Chicago, Chicago, IL 60612, USA

I.K. Schuller
Department of Physics, University of California—San Diego, La Jolla, CA 92093, USA

1 Introduction

Type II superconductors develop for intermediate magnetic fields superconducting vortices, which have been the focus of a rich field of research in both conventional and high temperature superconductivity. A central topic of these investigations has been the role of pinning, since this can determine a wide variety of static and dynamic phases and is also crucial for applications, which typically require vortex motion to be suppressed. One very fruitful approach towards investigating pinning phenomena is through the use of artificially fabricated periodic pinning arrays, which give rise to coherent pinning phenomena with well-ordered superconducting vortex lattices. In particular the use of magnetic nanostructures for such pinning arrays has been widely adopted [1], since they allow preparation of structures at length scales relevant to the superconducting vortex physics, such as the coherence length ξ and magnetic penetration length λ. Moreover, they offer additional flexibility in manipulating the vortex pinning through varying magnetization states [2–8]. For example, well-controlled magnetic particle arrays have been used for studying geometrical distortions of the vortex lattices through the use of rectangular arrays [9] and the rectification of vortex motion through asymmetrically shaped pinning centers [10–12].

This article focuses on two issues related to periodic superconducting vortex pinning with magnetic dot arrays; the role of size and magnetic configuration of the magnetic dots. From investigations of superconductors with periodic arrays of holes it is already known that the size of the pinning site can influence the behavior considerably. It was shown that for sufficiently large pinning sites multi-quanta vortices can be stabilized [13–15] and that the optimal size for the pinning center can be larger than the superconducting coherence length ξ, which determines the vortex core size [16]. However, with magnetic dots the situation may be more complex, since changing the magnetic dot size may also alter significantly the magnetization structure and hence the interplay between the magnetic dots and the superconductors. One particular interesting example are sufficiently large circular dots with small magnetic anisotropy, where the magnetization can form at low fields so-called magnetic vortex structures, since the magnetization curls up along the edges in order to avoid stray magnetic fields [17–20]. However, in the center of the magnetic vortex the magnetization points perpendicular to the magnetic dot in order to avoid a singularity. This magnetic vortex core has a diameter given by the magnetic exchange length, and therefore is typically a few nm in diameter [20–22]. As is shown further below, the presence or absence of such a magnetic vortex state changes the superconducting pinning properties of the magnetic dot array [8, 23].

2 Experimental

The arrays of magnetic dots were prepared with electron beam lithography and lift-off [24] on top of Si(100) substrates. An example of a magnetic dot structure indicating the exquisite control over size and placement of the dots is shown in Fig. 1. For the samples discussed in Sect. 3.1 magnetron sputter Ni magnetic dots with thicknesses ranging from 34–41 nm, diameters between 100 to 530 nm, and periodicities of either 400 or 600 nm were used. For the samples in Sect. 3.2 permalloy ($Ni_{80}Fe_{20}$) magnetic dots were deposited using electron beam evaporation with a thickness of 25 nm, 600-nm diameter, and 1-μm periodicity. After preparation, the magnetic dots were covered by continuous Nb films deposited either via molecular beam epitaxy (Sect. 3.1, thickness 56 nm) or sputter deposition (Sect. 3.2, thickness 100 nm). Subsequently, a four-point measurement bridge was defined in the Nb films with photolithography and reactive ion etching. The *dc* magnetoresistance was measured in a helium bath cryostat with variable angle θ of the field and the surface normal. Additionally for the magnetic dots used in Sect. 3.2 we measured the magnetic hysteresis loops for large arrays of uncovered magnetic dots using a superconducting quantum interference device (SQUID).

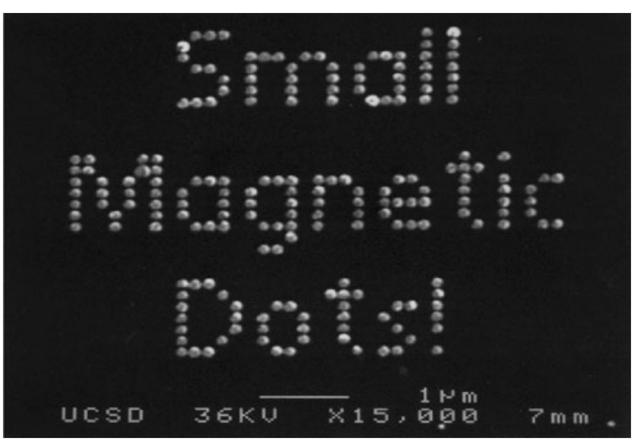

Fig. 1 Scanning electron micrograph of small magnetic Ni dot structure prepared with electron beam lithography and lift-off. Adapted from Ref. [36]

3 Results and Discussion

3.1 Varying Size and Separation

Figure 2 shows the magnetoresistance of a sample with 340-nm diameter Ni dots on a 400-nm square lattice measured at $T/T_c = 0.93$ and the field applied perpendicular to the thin film plane ($\theta = 0°$). There are several periodically spaced (125 Oe) resistivity minima. With increasing field the density of the superconducting vortices increases and at each minimum the ratio of the vortex to pinning site density is an integer [25]. Hence for the case of a square lattice each mth matching field is given by [26, 27]:

$$H_m = m\frac{\Phi_0}{a^2}, \tag{1}$$

where $\Phi_0 = 10.7\ \mathrm{G/\mu m^2}$ is the magnetic flux quantum, and a is the lattice constant of the square lattice. The commensurability between the vortex lattice and the pinning arrays gives rise to a geometric matching [28, 29], which is schematically shown in Fig. 2(b) for the case where at most one vortex is trapped per pinning site.

When the applied magnetic field is tilted away from the surface normal, the periodicity of the matching fields ΔH increases, as shown in Fig. 3(a). This increase is well described by $\Delta H = H_1/\cos\theta$ (see Fig. 3(b)), which indicates that only the perpendicular field component is relevant for the periodicity of the superconducting vortex lattice [25]. Another important aspect is that the data in Fig. 3(a) are symmetric with respect to positive and negative fields without any observable hysteretic behavior. This may be expected since the magnetic behavior of the dots should not have any hysteresis in this geometry. Applying the magnetic field mostly perpendicular to the substrate surface, which is the magnetic hard axis direction, results in reversible hysteresis loops with very little, if any, hysteresis.

The periodic pinning found in the magnetoresistance (see Fig. 2(a)) is also reflected in the magnetic field dependence of the critical current [4, 30]. Using a voltage criterion of 20 μV/cm we determined the magnetic field dependence of the critical currents for various different samples with dot sizes ranging from 110 nm to 340 nm, each on a regular square lattice with 400-nm periodicity. The sample with 340-nm dots exhibits critical current maxima with the same field periodicity as found for the minima

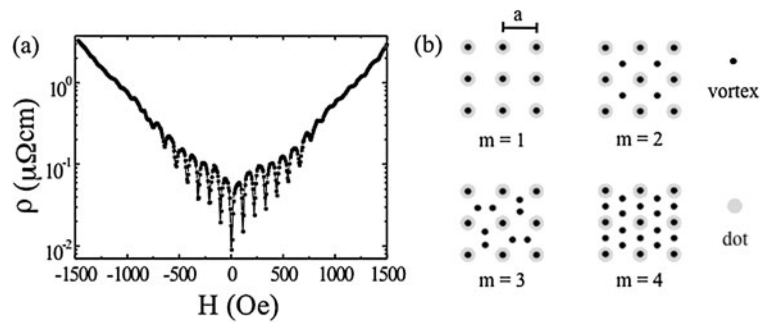

Fig. 2 (**a**) Magnetoresistance for a sample with 340-nm diameter Ni dots on a 400-nm square lattice. (**b**) Schematic of various superconducting vortex arrangements for increasing matching fields corresponding to integer multiples of the ratio of vortex-to-pinning site densities. Adapted from Ref. [36]

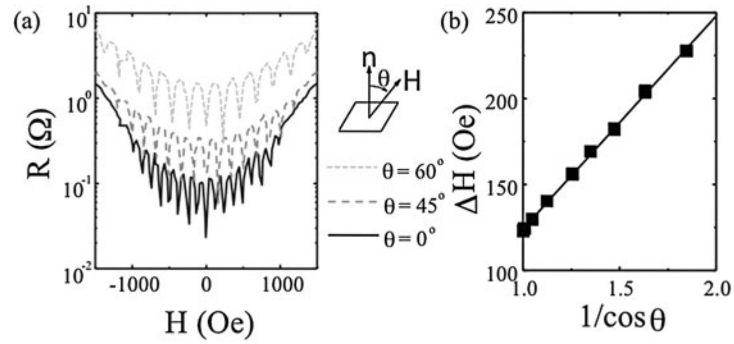

Fig. 3 (**a**) Magnetoresistance as a function of angle θ of the magnetic field H with respect to the surface normal n.
(**b**) Angular dependence of the magnetic field periodicity observed in (**a**). Adapted from Ref. [36]

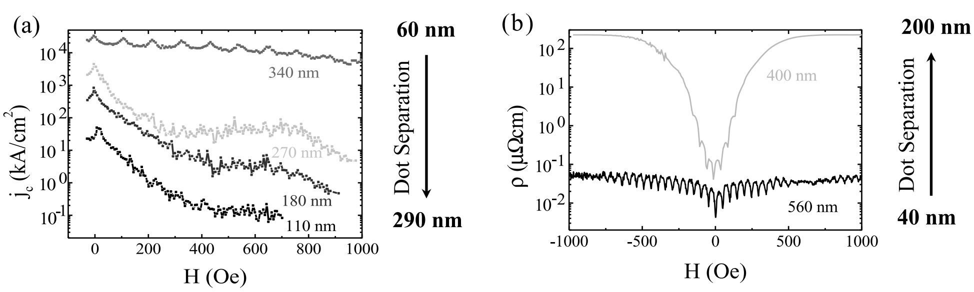

Fig. 4 (**a**) Critical current as a function of field for Ni dots with varying diameter and a fixed 400-nm square lattice.
(**b**) Magnetoresistance of 400-nm and 560-nm diameter Ni dots on a 600-nm square lattice. Adapted from Ref. [4]

in the magnetoresistance. Interestingly the period pinning is absent for the smaller dots. This behavior is also reflected in the magnetoresistance of all these samples where the periodic pinning features in the magnetoresistance are fewer and less pronounced for the smaller dots [4]. Such significant variation with dot size is somewhat surprising, since all the dot diameters are larger than the superconducting coherence length, which we estimate from the upper critical field at the measurement temperature to be about $\xi \approx 58$ nm.

In order to investigate, whether the diameter of the dots is the crucial parameter for the periodic pinning features, we also prepared Ni dot arrays with a larger periodicity of 600 nm. The magnetoresistance for samples with 400- and 560-nm diameter are shown in Fig. 4(b). Clearly, the magnetoresistance of the 340-nm dots with 400-nm periodicity is qualitatively different from the 400-nm dots and the periodic pinning effects are again more pronounced for the 560-nm dots. It is important to note that while the dots size is increased, their edge-to-edge distance decreases for equal periodicity. In particular, for the 340-nm dots with 400-nm periodicity and for the 560-nm dots with 600-nm periodicity, the edge-to-edge separation is 60 and 40 nm, respectively, and therefore comparable to the superconducting coherence length. A similar crossover as a function of dot separation has also been observed for hole arrays in superconductors [16]. This suggests that as the dot separation becomes smaller than the superconducting coherence length the system changes from a periodic pinning regime, where the magnetoresistance is dominated by vortex motion, to a superconducting network behavior with each loop containing a quantized magnetic flux resulting in Little–Parks oscillations [31, 32]. This interpretation is also supported by theoretical simulations, which suggest that the critical current peaks of similar magnitude, as observed for the 340-nm Ni dots shown in Fig. 3(a), are indicative of multivortex pinning [33]. In short, the size plays little role for the periodic pinning, but the separation between pinning dots is important.

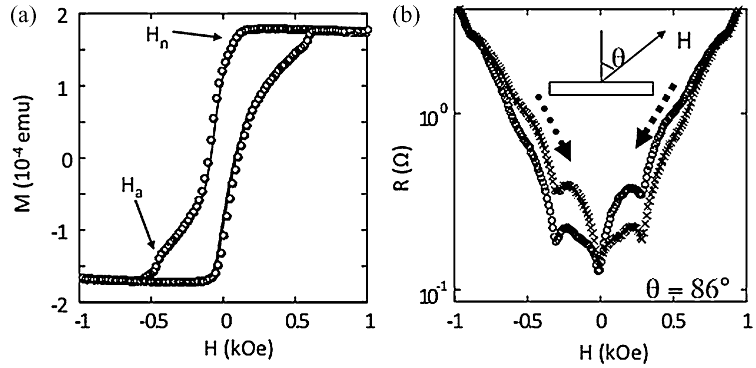

Fig. 5 (**a**) Magnetic hysteresis loop measured at 8.27 K with an in-plane ($\theta = 90°$) magnetic field for 600-nm diameter permalloy dots on a 1-μm square lattice. (**b**) Magnetoresistance measured at the same temperature and $\theta = 86°$. *Circles* indicate measurements with decreasing fields, while *crosses* indicate increasing fields. Adapted from Ref. [8]

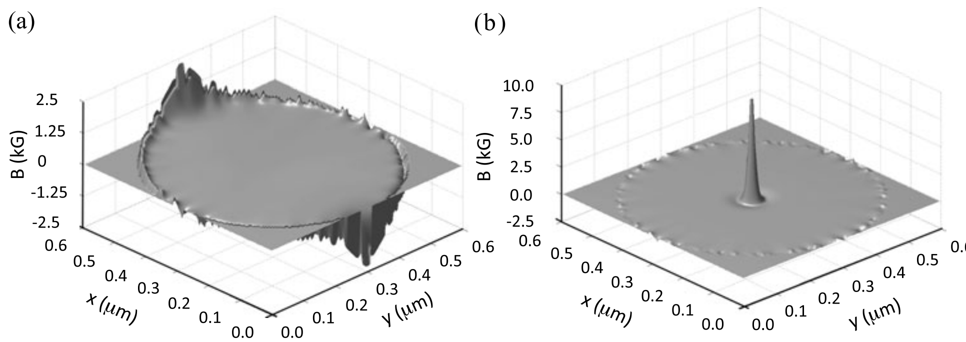

Fig. 6 Perpendicular magnetic stray field distribution calculated by micromagnetic simulation for a magnetic dot in a saturated state (**a**) and with a vortex magnetization state (**b**). Adapted from Ref. [8]

3.2 Varying the Magnetization State

Sufficiently large magnetic structures can accommodate a wide variety of magnetic states and thus naturally the question arises, how they may influence the vortex pinning. One particularly interesting example is the formation of magnetic vortices, where the reversal of magnetization occurs in two distinct steps. This is shown in Fig. 5(a) for 600-nm permalloy dots. As the magnetic field is reduced from saturation, close to zero applied field there is a large change in the magnetization associated with the nucleation of magnetic vortices at H_n, which is followed by reversible magnetization changes due to the magnetic vortex displacement, followed by another distinct step at H_a due to the annihilation of the magnetic vortices. The hysteresis in the central part of the loop is an artifact produced because a large ensemble of dots with a distribution of nucleation fields is measured. Minor loops of the same sample show no hysteresis [8] and individual dots show well-defined critical fields with complete reversible behavior in the vortex state [34].

Figure 5(b) shows the magnetoresistance at $T/T_c = 0.99$ for 100-nm thick Nb film covering the same permalloy dot array while applying the magnetic field at $\theta = 86°$ with respect to the surface normal. Note that for this angle the magnitude of the in-plane component of the field is nearly identical (99.8 %) to the entire applied magnetic field, while the out-of-plane component is still a sizable fraction (7.0 %). There are still well-defined resistivity minima, consistent with Eq. (1), if only the out-of-plane field component is considered. However, unlike in the cases before (Figs. 2 and 3) where the field was predominantly out-of-plane, the magnetoresistance shows a pronounced hysteretic behavior in the same field regions, where the magnetization reversal also shows hysteretic behavior. Comparison with the magnetic measurements in Fig. 5(a) shows that the magnetization minima are significantly lower for the field intervals, where a magnetic vortex is formed in the magnetic dot compared to the case where the magnetization is mostly saturated. This clearly shows that the presence of a magnetic vortex significantly enhances the pinning of superconducting vortices.

The reason for this enhanced pinning is that although the overall stray field is reduced for a magnetic dot in the vortex state, locally the stray field can be substantially enhanced by the presence of the perpendicularly magnetized vortex core. Conversely, the stray field of a magnetic dot in a saturated state is mostly in-plane and does not necessarily penetrate the superconducting film. This is shown in Fig. 6(b), which shows the perpendicular component of the external stray magnetic field (≈10 kG) for the magnetic vortex state and the saturated state, as determined by micromagnetic simulation [8]. These simulations imply that the stray field of the magnetic vortex core can locally be one order of magnitude bigger than for the saturated state, and can effectively suppress superconductivity by exceeding the upper critical field close to T_c. A similar suppression of superconductivity has also been observed in other systems, which combine magnetic vortices with superconductors [23].

4 Conclusions

In the almost 40 years since superconducting vortex pinning via magnetic structures has been first suggested [35], this research topic has resulted in a wide variety of activities, especially during the past decade (see e.g., Ref. [1] for a recent detailed review). Here we showed the influence of two issues; size and magnetic configuration. Reducing the separation between adjacent pinning centers can result in a crossover from a weak pinning regime dominated by coherent vortex motion to a superconducting wire network regime, where the periodic resistivity minima can extend to very high matching fields. Furthermore, introducing locally very high magnetic fields, i.e., through the formation of magnetic vortex cores, offers novel opportunities to control superconducting vortex pinning. Therefore it can be expected that the research of vortex physics in ferromagnetic/superconducting hybrid systems will maintain its vitality far into the second century of superconductivity!

Acknowledgements Part of this work was done in collaboration with L. Fumagalli, N. Jahedi, J. Martín, M. Vélez, J.C. Sautner, J. Vicent, S.D. Bader, J.E. Pearson, and G. Mihajlović. Work at Argonne was supported by the U.S. Department of Energy, Office of Science, Basic Energy Sciences, under contract No. DE-AC02-06CH11357. Work at the University of Illinois at Chicago was supported by the U.S. NSF, grant ECCS-0823813. Work at the University of California—San Diego was supported by the U.S. NSF.

References

1. Vélez, M., Martín, J.I., Villegas, J.E., Hoffmann, A., González, E.M., Vicent, J.L., Schuller, I.K.: J. Magn. Magn. Mater. **320**, 2547 (2008)
2. Morgan, D.J., Ketterson, J.B.: Phys. Rev. Lett. **80**, 3614 (1998)
3. van Bael, M.J., Temst, K., Moshchalkov, V.V., Bruynseraede, Y.: Phys. Rev. B **59**, 14674 (1999)
4. Hoffmann, A., Prieto, P., Schuller, I.K.: Phys. Rev. B **61**, 6958 (2000)
5. Milošević, M.V., Yampolskii, S.V., Peeters, F.M.: Phys. Rev. B **66**, 174519 (2002)
6. van Bael, M.J., Lange, M., Raedts, S., Moshchalkov, V.V., Grigorenko, A.N., Bending, S.J.: Phys. Rev. B **68**, 014509 (2003)
7. Villegas, J.E., Li, C.-P., Schuller, I.K.: Phys. Rev. Lett. **99**, 227001 (2007)
8. Hoffmann, A., Fumagalli, L., Jahedi, N., Autner, J.C., Pearson, J.E., Mihajlović, G., Metlushko, V.: Phys. Rev. B **77**, 060506(R) (2008)
9. Martín, J.I., Vélez, M., Hoffmann, A., Schuller, I.K.: Phys. Rev. Lett. **83**, 1022 (1999)
10. Villegas, J.E., Savel'ev, S., Nori, F., Gonzalez, E.M., Anguita, J.V., García, R., Vicent, J.L.: Science **302**, 1188 (2003)
11. Silhanek, A.V., Gillijns, W., Moshchalkov, V.V., Metlushko, V., Illic, B.: Appl. Phys. Lett. **89**, 182505 (2006)
12. Silhanek, A.V., Gilijns, W., Moshchalkov, V.V., Metlushko, V., Gozzini, F., Illic, B., Uhlig, C., Unguris, J.: Appl. Phys. Lett. **90**, 182501 (2007)
13. Bart, M., Metlushko, V.V., Jonckheere, R., Moshchalkov, V.V., Bruynseraede, Y.: Phys. Rev. Lett. **74**, 3269 (1995)
14. Bezryadin, A., Pannetier, B.: J. Low Temp. Phys. **102**, 73 (1996)
15. Moshchalkov, V.V., Baert, M., Metlushko, V.V., Rossel, E., van Bael, M.J., Temst, K., Jonckheere, R., Bruynseraede, Y.: Phys. Rev. B **54**, 7385 (1996)
16. Moshchalkov, V.V., Baert, M., Metlushko, V.V., Rossel, E., van Bael, M.J., Temst, K., Jonckheere, R., Bruynseraede, Y.: Phys. Rev. B **57**, 3615 (1998)
17. Cowburn, R.P., Koltsov, D.K., Adyeye, A.O., Welland, M.E., Tricker, D.M.: Phys. Rev. Lett. **83**, 1042 (1999)
18. Shinjo, T., Okuno, T., Hassdorf, R., Shigeto, K., Ono, T.: Science **289**, 930 (2000)
19. Guslienko, K.Y., Novosad, V., Otani, Y., Shima, H., Fukamichi, K.: Phys. Rev. B **65**, 024414 (2001)
20. Wachowiak, A., Wiebe, J., Bode, M., Pietsch, O., Morgenstern, M., Wiesendanger, R.: Science **298**, 577 (2002)
21. Miltat, J., Thiaville, A.: Science **298**, 555 (2002)
22. Roshchin, I.V., Li, C.-P., Suhl, H., Battle, X., Roy, S., Sinha, S.K., Park, S., Pynn, R., Fitzsimmons, M.R., Mejia-Lopez, J., Altbir, D., Romero, A.H., Schuller, I.K.: Europhys. Lett. **86**, 67008 (2009)
23. Villegas, J.E., Li, C.-P., Schuller, I.K.: Phys. Rev. Lett. **99**, 227001 (2007)
24. Martín, J.I., Jaccard, Y., Hoffmann, A., Nogués, J., George, J.M., Vicent, J.L., Schuller, I.K.: J. Appl. Phys. **84**, 411 (1998)
25. Martín, J.I., Vélez, M., Nogués, J., Schuller, I.K.: Phys. Rev. Lett. **79**, 1929 (1997)
26. Fiory, A.T., Hebard, A.F., Somekh, S.: Appl. Phys. Lett. **32**, 73 (1978)
27. Jaccard, Y., Martín, J.I., Cyrille, M.-C., Vélez, M., Vicent, J.L., Schuller, I.K.: Phys. Rev. B **58**, 8232 (1998)
28. Harada, K., Kamimura, O., Kasai, H., Matsuda, T., Tonomura, A., Moshchalkov, V.V.: Science **274**, 1167 (1996)
29. Reichhardt, C., Olsen, C.J., Nori, F.: Phys. Rev. B **57**, 7937 (1998)
30. Jaccard, Y., Martín, J.I., Cyrille, M.-C., Vélez, M., Vicent, J.L., Schuller, I.K.: Phys. Rev. B **58**, 8232 (1998)
31. Pannetier, B., Chaussy, J., Rammal, R., Villegier, J.C.: Phys. Rev. Lett. **53**, 1845 (1984)
32. Little, W.A., Parks, R.: Phys. Rev. A **133**, A97 (1964)
33. Reichhardt, C., Zimanyi, G.T., Scalettar, R.T., Hoffmann, A., Schuller, I.K.: Phys. Rev. B **64**, 052503 (2001)
34. Mihajlović, G., Patrick, M.S., Pearson, J.E., Novosad, V., Bader, S.D., Field, M., Sullivan, G.J., Hoffmann, A.: Appl. Phys. Lett. **96**, 112501 (2010)
35. Autler, S.H.: J. Low Temp. Phys. **9**, 241 (1972)
36. Hoffmann, A.: Ph.D. thesis. University of California, San Diego (1999)